DRIE TRENCHES AND FULL-BRIDGES DESIGN FOR SENSITIVITY IMPROVEMENT OF MEMS SILICON THERMAL WIND SENSOR

Yizhou Ye, Zhenxiang Yi, Ming Qin and Qing-an Huang*
Key Laboratory of MEMS of the Ministry of Education, Southeast University, Nanjing, CHINA

ABSTRACT

In this paper, a micromachined silicon thermal wind sensor with improved sensitivity is demonstrated. Deep reactive ion etching (DRIE) trenches are fabricated to suppress the lateral heat conduction between the heater and the thermistors. Moreover, two Wheatstone full-bridges consisting of eight thermistors are designed to increase the output voltage by 50%. Based on these two methods, the sensitivity of the micromachined wind sensor can be improved remarkably, which is verified by the experiments. The results show that the measurement wind speed range can be up to 33m/s in constant voltage (CV) mode with the initial heating power of 256mW. The sensitivity is measured to be 29.37mV/ms^{-1} at the wind speed of 3.3m/s, achieving an improvement of about 226%, compared with the traditional wind sensor. The results also show that wind direction in a full range of 360° can be determined with an accuracy of ±5°.

INTRODUCTION

Micromachined silicon thermal wind sensor has been considered as one of the most significant implementations of thermal flow sensor, and has been investigated extensively due to simple structure, compact size, fast response and high sensitivity [1-5]. According to the different sensing surfaces, micromachined silicon thermal wind sensor can be categorized into two kinds: front surface sensing and back surface sensing. The former relies on the front surface of the sensor to interact with the airflow [6-10]. These sensors are usually fabricated on the micromembranes to minimize the heat loss through the substrate, and the heaters and thermistors of them are directly exposed to the airflow. Therefore, these sensors excel in high sensitivity and low power consumption. However, in practical applications, the chip is easy to be polluted by particles in the air and the packaging is indispensable. The exposure of the front surface makes the packaging difficult to be deployed. Moreover, the micromembranes fabricated by anisotropic etching of silicon substrate cannot survive vibration or mechanical shocks. Above all, the bonding wires between the sensor chip and PCB board are easy to be damaged by front surface sensing. In order to solve these problems, back surface sensing is proposed [11-13]. These sensors achieve thermal contact with the airflow via the backside of the chip. They are fabricated on silicon substrate and then mounted onto PCB board to implement self-package. The self-package allows standard wire bonding to be applied, and, hence the risk of the wires damaged by the airflow is eliminated. However, due to the large thermal conductivity of silicon substrate, the magnitude of the airflow induced temperature difference is quite small, resulting in low sensitivity and high power consumption.

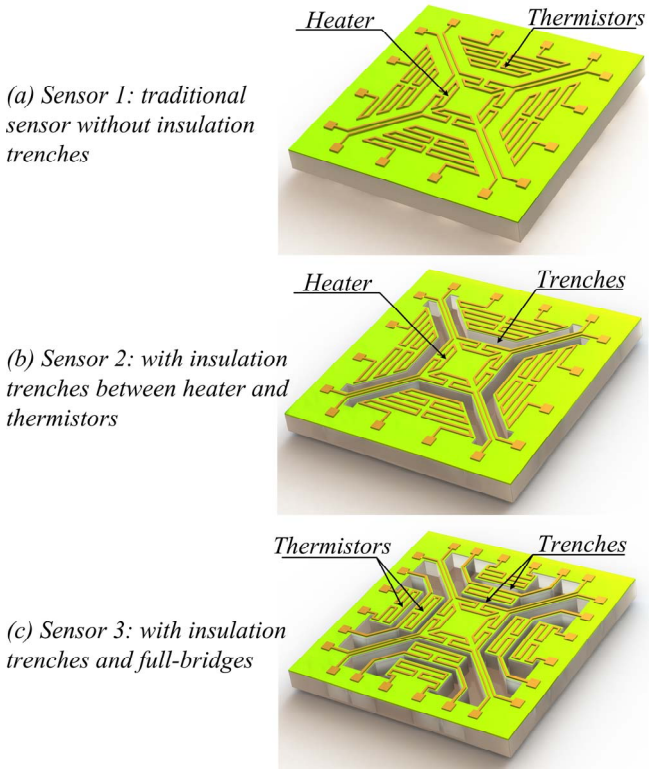

(a) Sensor 1: traditional sensor without insulation trenches

(b) Sensor 2: with insulation trenches between heater and thermistors

(c) Sensor 3: with insulation trenches and full-bridges

Figure 1: Perspective view of the micromachined silicon thermal wind sensors.

In this paper, a back surface sensing wind sensor with improved sensitivity is demonstrated. In this device, DRIE trenches are fabricated between the heater and thermistors to reduce the lateral heat loss. Furthermore, eight thermistors symmetrically placed in four directions around the heater are configured to two Wheatstone full-bridges. Based on these two combined designs, the proposed micromachined silicon thermal wind sensor obtains an improved sensitivity, compared with the traditional one.

DESIGN AND PRINCIPLE

Figure 1(a) shows the perspective view of the traditional micromachined silicon thermal wind sensor, consisting of heater, four thermistors and silicon substrate. The heater composed of four resistors is located in the center of the chip. The four-resistor configuration is to enable the heating of the sensor to be balanced in two perpendicular directions. Four thermistors are arranged symmetrically around the heater in two perpendicular directions, and measure the temperature change resulted by the wind. When a voltage is applied, the heat distribution field is symmetrical for the condition of no wind. When the airflow passes over the backside of the chip, the heat is taken from upstream to downstream. Hence, the

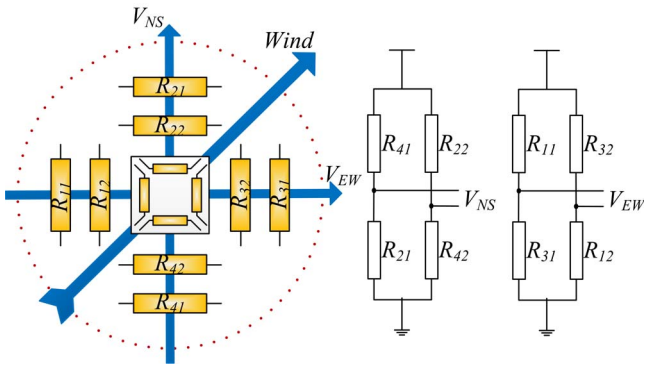

Figure 2: Schematic of the full-bridges for calorimetric principle measurement.

upstream temperature decreases while the downstream temperature increases. Two Wheatstone half-bridges are designed to measure the change of the four thermistors. As a result, the wind information can be resolved by the output DC voltages.

In order to reduce the lateral heat loss in the chip, DRIE technology is utilized to fabricate the insulation trenches between the heater and the thermistors, as shown in figure 1(b). On this basis, as shown in figure 1(c), two thermistors are located at different distance from the central heater in one direction, and full-bridges technology is utilized to further enhance the performance of the wind sensor. Figure 2 gives the equivalent circuit of the proposed design. Each four thermistors in relative directions are configured to Wheatstone full-bridge. The full-bridge configuration has almost two times the output of the traditional half-bridge formed by two thermistors and two discrete resistors.

FABRICATION AND PACKAGING

The proposed silicon thermal wind sensor was fabricated by a standard MEMS process. As shown in figure 3, the process mainly consists of six steps, namely: (1) thermal oxidation; (2) lithographing Ni; (3) sputtering Ni; (4) lift-off; (5) patterning Al; (6) etching trenches with DRIE.

In order to reduce the lateral heat conduction effect, the process was started with a double-side-polished 4 inch n-type (111) silicon wafer with a thickness of 250 μm. A 200 nm-thickness SiO_2 layer was thermally grown on the silicon substrate. The SiO_2 layer on the front surface realized electrical isolation between the silicon substrate and the active element of the sensor, while the SiO_2 on the backside was utilized to prevent the sensing surface from undesired media, and make sure the long-term stability of the device. Next, 2 μm-thickness AZ5214 photoresist was spin-coated and patterned on the SiO_2 layer. A sputtering process was then performed to deposit Ni with a thickness of 200 nm. After that, the wafer was soaked in acetone to lift off the unwanted Ni, forming the heaters and thermistors. Then, a 400 nm-thickness Al film was deposited and patterned on the substrate to obtain the pads for wire bonding. Finally, the insulation trenches were fabricated via DRIE technology and the depth was about 200 μm.

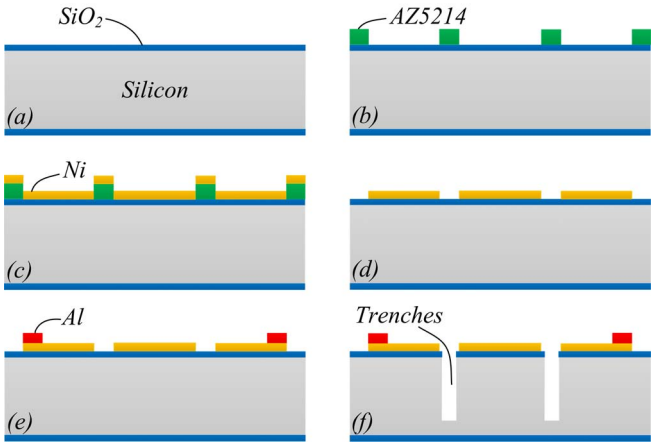

Figure 3: Fabrication process of the silicon thermal wind sensor: (a) thermal oxidation; (b) lithographing Ni; (c) sputtering Ni; (d) lift-off; (e) patterning Al; (f) etching trenches with DRIE.

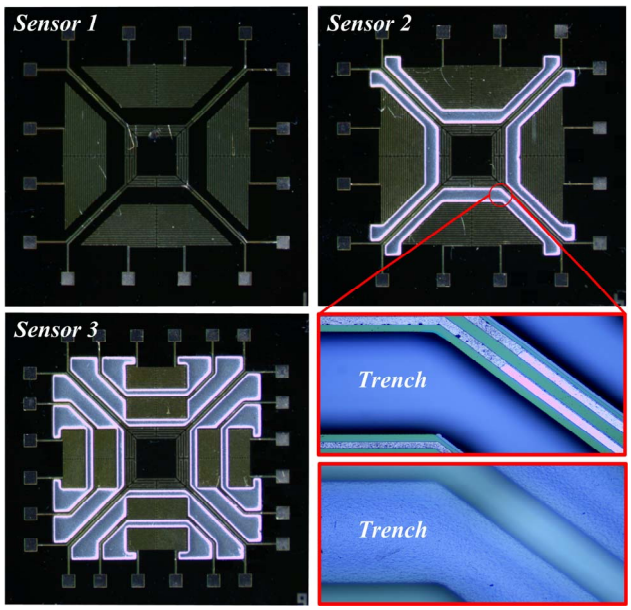

Figure 4: Photographs of the fabricated silicon thermal wind sensors, and the trenches.

Figure 4 shows the photographs of the fabricated silicon thermal wind sensors. The overall dimension of the sensor chip is 6mm×6mm×0.25mm. The resistances of the fabricated heaters and thermistors are 250 Ω and 2 kΩ at room temperature, respectively. The temperature coefficient of the Ni resistance is about 4500 ppm in the range of -10 ℃ to 50 ℃.

Moreover, the self-package is generally utilized in the back surface sensing because of its simple implementation and low cost. Figure 5(a) shows the cross-section view of the self-packaged traditional wind sensor. The heaters and thermistors were fabricated on the front surface of the chip, while the back surface was utilized as the packaging surface as well as sensing surface. The standard bonding wires of the sensor were directly applied between the front surface and

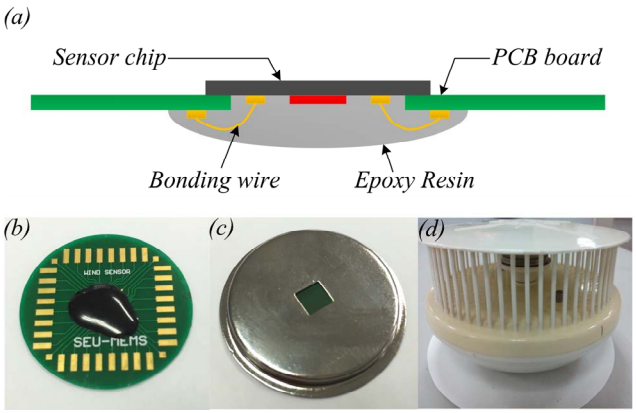

Figure 5: The self-package of the wind sensor. (a) Schematic cross-section view of the packaged traditional wind sensor. Photograph of the fabricated wind sensor (b) after wire bonding and sealing with epoxy resin; (c) glued to the aluminum frame; and (d) packaged in the protection shell.

the PCB board. Epoxy resin with low thermal conductivity was utilized to protect the bonding wires and the front surface of the sensor from the poor environment conditions. Then an aluminum frame was glued to the PCB board to protect the chip. Finally, the sensor was installed to a protection shell to work at outdoors environment. Figure 5 also gives the photographs of the fabricated wind sensor after wire bonding and sealing with epoxy resin, glued to the aluminum frame, and packaged in the protection shell.

EXPERAMENTS AND DISCUSSIONS

Fabricated sensors were installed in a laminar flow wind tunnel. The wind tunnel covers wind speed up to 33m/s and a full range of 360° for wind direction measurement. In the measurement, two low-offset instrument amplifiers AD623 with about 200 times the amplification were designed to amplify and modify the output voltages of the Wheatstone bridges, and the output analog signals of the amplifiers AD623 were digitalized by a microprocessor. The microprocessor received the signal and computed the magnitude and direction of the wind. Finally, the wind information was displayed on a LCD.

The wind speed was approximated by $sqrt(V_{NS}^2+V_{EW}^2)$. When the sensors operated in constant voltage (CV) mode and the initial heating power was 256mW, the output voltages of the calorimetric systems are recorded in figure 6. It can be observed that, after fabricating the insulation trenches with DRIE technology between the heater and thermistors, the output signal curve of the sensor significantly rises. Moreover, the combination of the insulation trenches and full-bridges design further enhances the performance of the sensor, as the output signal curve of sensor 3 shows. Especially, the sensitivity of the sensor at a specific wind speed is given by the slope of the output signal curve at that speed. In this work, the sensitivities of the sensors were given at 3.3m/s. The measured sensitivity is about 9.01mV/ms^{-1}, 16.37mV/ms^{-1}, and 29.37mV/ms^{-1} for sensor 1, 2, and 3, respectively. It is demonstrated that the

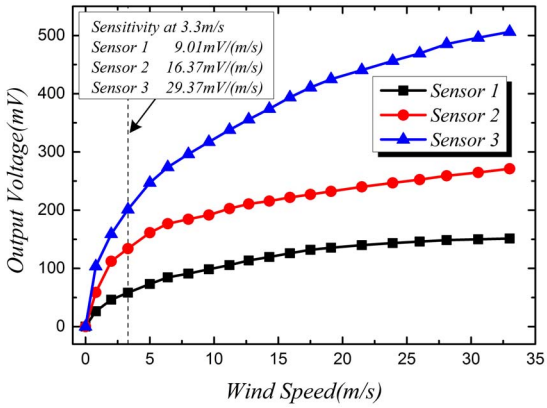

Figure 6: Output voltages of calorimetric system for wind speed measurement at initial heating power 256mW.

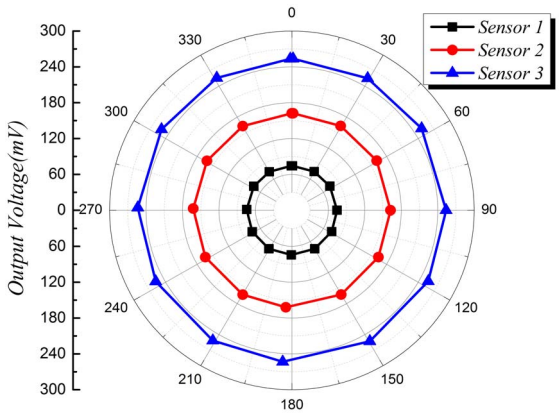

Figure 7: Output voltage V_{NS} for wind direction measurement in a full range of 360° at 5m/s.

sensitivity can be improved by 82% with insulation trenches design and further by 226% based on the combination of insulation trenches and full-bridges design.

Figure 7 shows the measured bridge output V_{NS} of the calorimetric system at the wind speed 5m/s with an interval of 30°. The output voltage V_{NS} varies regularly with the change of wind direction. Moreover, it can be observed that the vertical axis in figure 7 shows the ratio of the sensitivity of the sensor 1, 2, and 3.

In order to evaluate the measurement accuracy of the proposed wind sensor, the packaged sensor and the conditioning circuit were calibrated in the wind tunnel. The wind speed was calculated by the linear interpolation of $sqrt(V_{NS}^2+V_{EW}^2)$, and the wind direction was computed by $arctan(V_{EW}/V_{NS})$. After calibration, the complete system was installed in the wind tunnel to verify the accuracy of the sensor by comparing the calculated speeds and directions with the actual speeds and directions. Figure 8 shows the measurement errors for the wind speeds up to 33m/s, and figure 9 shows the errors for wind directions at 5m/s. It can be observed that for the wind speeds less than 25m/s, the errors of the sensor are less than 0.4m/s while the errors increase to about 0.6m/s at 33m/s. The direction errors for this sensor are less than 5 degrees when the wind direction changes from 0° to 360°.

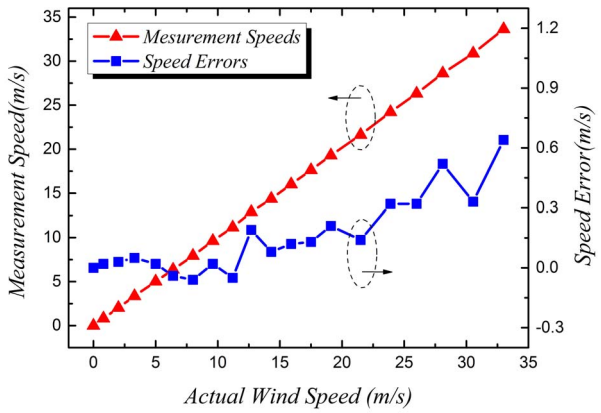

Figure 8: Measurement errors of wind speed up to 33m/s.

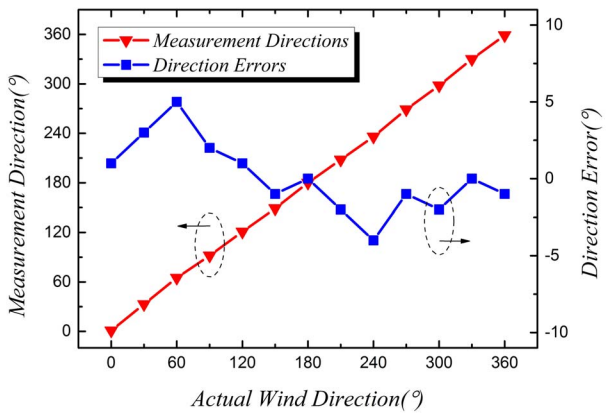

Figure 9: Measurement errors of wind direction at 5m/s.

CONCLUSION

A high-sensitivity, robust and self-packaged micromachined 2-D silicon thermal wind sensor has been presented, fabricated and tested. Unlike the traditional back surface sensing, the proposed sensor utilizes the DRIE technology to etch insulation trenches between the heater and thermistors, significantly suppressing the unwanted lateral heat conduction in the chip. Moreover, two Wheatstone full-bridges forming by eight thermistors are also employed to enable about 50% increase of the sensitivity compared with four thermistors. Based on the DRIE trenches and full-bridges design, the micromachined silicon thermal wind sensor achieves a remarkable sensitivity improvement. The wind speeds were measured up to 33m/s with an accuracy of 0.4m/s at the low speed ranges and 0.6m/s at the high speed ranges. Wind directions can be determined in a full range of 360 degrees with a maximum error of 5 degrees. The proposed micromachined silicon thermal wind sensor can be used in some applications that require high sensitivity and high reliability.

REFERENCES

[1] A. F. P. van Putten, M. J. A. M. van Putten, and M. H. P. M. van Putten, "Silicon thermal anemometry: Developments and applications," *Meas. Sci. Technol.*, vol. 7, no. 10, pp. 1360–1377, Oct. 1996.

[2] N. T. Nguyen, "Micromachined flow sensors—A review," *Flow Meas. Instrum.*, vol. 8, no. 1, pp. 7–16, Mar. 1997.

[3] H. Baltes, O. Paul, and O. Brand, "Micromachined thermally based CMOS microsensors," *Proc. IEEE*, vol. 86, no. 8, pp. 1660–1678, Aug. 1998.

[4] J. T. W. Kuo, L. Yu, and E. Meng, "Micromachined thermal flow sensors—A review," *Micromachines*, vol. 3, no. 3, pp. 550–573, Mar. 2012.

[5] Y. Zhu, B. Chen, M. Qin, and Q.-A. Huang, "2-D micromachined thermal wind sensors—A review," *IEEE Internet Things J.*, vol. 1, no. 3, pp. 216–232, Jun. 2014.

[6] N. Sabaté, J. Santander, L. Fonseca, I. Gràcia, and C. Cané, "Multi-range silicon micromachined flow sensor," *Sens. Actuators A, Phys.*, vol. 110, nos. 1–3, pp. 282–288, Feb. 2004.

[7] S. Kim, T. Nam, and S. Park, "Measurement of flow direction and velocity using a micromachined flow sensor," *Sens. Actuators A, Phys.*, vol. 114, nos. 2–3, pp. 312–318, 2004.

[8] J. B. Sun, M. Qin, and Q. A. Huang, "Flip-chip packaging for a two dimensional thermal flow sensor using a copper pillar bump technology," *IEEE Sensors J.*, vol. 7, no. 7, pp. 990–995, Jul. 2007.

[9] R. J. Adamec, and D. V. Thiel, "Self heated thermo-resistive element hot wire anemometer," *IEEE Sensors J.*, vol. 10, no. 4, pp. 847-848, Apr. 2010.

[10] Z. Dong, J. Chen, Y. Qin, M. Qin, and Q. A. Huang, "Fabrication of a micromachined two-dimensional wind sensor by Au-Au wafer bonding technology," *J. Microelectromech. Syst.*, vol. 21, no. 2, pp. 476–475, Apr. 2012.

[11] B. W. Van Oudheusden, "Silicon thermal flow sensor with a two-dimensional direction sensitivity," *Meas. Sci. Technol.*, vol. 1, no. 7, pp. 565–575, Jul. 1990.

[12] D. H. Gao, M. Qin, H. Y. Chen, and Q. A. Huang, "A self-packaged thermal flow sensor by CMOS MEMS technology," in *Proc. 3rd IEEE Conf. Sensors*, Vienna, Austria, 2004, pp. 879-883.

[13] J. Wu, C.P.L. van Vroonhoven, C. Youngcheol, and K.A.A. Makinwa, "A 25mW CMOS sensor for wind and temperature measurement," in *Proc. 10th IEEE Conf. Sensors*, Limerick, Ireland, 2011, pp. 1261-1264.

CONTACT

*Ming Qin, tel: +86-25-83792632; mqin@seu.edu.cn